Can fracture orientation and intensity be detected from seismic data? Woodford Formation, Anadarko Basin, Oklahoma investigation

Marianne Rauch-Davies[1], David Langton[1], Michael Bradshaw[2], Allon Bartana[2], Dan Kosloff[2], Jeff Codd[2], David Kessler[2], Jamie Rich[3], and Gary Margrave[4]

https://doi.org/10.1190/tle38020144.1.

Abstract

With readily available wide-azimuth, onshore, 3D seismic data, the search for attributes utilizing the azimuthal information is ongoing. Theoretically, in the presence of ordered fracturing, the seismic wavefront shape changes from spherical to nonspherical with the propagation velocity being faster parallel to the fracturing and slower perpendicular to the fracture direction. This concept has been adopted and is used to map fracture direction and density within unconventional reservoirs. More specifically, azimuthal variations in normal moveout velocity or migration velocity are often used to infer natural fracture orientation. Analyses of recent results have called into question whether azimuthal velocity linked to intrinsic azimuthal velocity variations can actually be detected from seismic data. By use of 3D orthorhombic anisotropic elastic simulation, we test whether fracture orientation and intensity can be detected from seismic data. We construct two subsurface models based on interpreted subsurface layer structure of the Anadarko Basin in Oklahoma. For the first model, the material parameters in the layers are constant vertically transverse isotropic (VTI) in all intervals. The second model was constructed the same way as the base model for all layers above the Woodford Shale Formation. For the shale layer, orthorhombic properties were introduced. In addition, a thicker wedge layer was added below the shale layer. Using the constructed model, synthetic seismic data were produced by means of 3D anisotropic elastic simulation resulting in two data sets: VTI and orthorhombic. The simulated data set was depth migrated using the VTI subsurface model. After migration, the residual moveouts on the migrated gathers were analyzed. The analysis of the depth-migrated model data indicates that for the typical layer thicknesses of the Woodford Shale layer in the Anadarko Basin, observed and modeled percentage of anisotropy and target depth, the effect of intrinsic anisotropy is too small to be detected in real seismic data.

Introduction

Substantial financial resources are being spent in acquiring and processing azimuthal seismic data. This is routinely followed by making business decisions based on the interpretation that any measured azimuthal normal moveout velocity (V_{NMO}) is directly related to fracture orientation and intensity. The ability to detect variations in fracture orientation and intensity in unconventional reservoirs has become a primary geophysical goal because it is desirable to map those features prior to drilling. Seismic data are well suited for this task as they provide both broad spatial coverage and azimuthal information.

Early approaches to azimuthal V_{NMO} used unmigrated data and depended on small dips. Lynn (2007, 2011) demonstrates that sectoring of data made the inversion for layer anisotropy properties unstable. Since then, approaches using offset vector tile migration have become standard. This allows preservation of azimuthal information through migration, suppressing the influence of dip on azimuthal V_{NMO} variations. Recent research has raised more questions on the connection between azimuthal V_{NMO} and intrinsic anisotropy. Belguermi et al. (2016) show that depth migration substantially reduces the effect of azimuthal V_{NMO}. Rich et al. (2016) show that there is a strong correlation between structural orientation and V_{NMO} azimuths. Both suggest that velocity heterogeneity may have stronger influence on V_{NMO} than intrinsic layer anisotropy. Rauch-Davies and Sutherland (2016) present results from a processing benchmark employing four different vendor groups (Figure 1). Analysis of the results clearly shows that the mapped velocity variation with azimuth did not agree with the known fracture framework in the reservoir unit. Furthermore, the various groups' results were not in agreement with each other. The need to investigate the ability to infer detailed fracture information from wide-azimuth seismic became evident.

The work presented here attempts to address the question of whether it is feasible to detect fracture orientation from azimuthal moveouts obtained from vertically transverse isotropic (VTI) depth-migrated gathers. For this purpose, an orthorhombic anisotropic elastic 3D simulation project was initiated. The subsurface model parameters used in the simulation project were similar to those estimated from the original real data benchmark data set (Rauch-Davies and Sutherland, 2016), and the formation horizons were taken from the interpretation of that real depth data set. The key Woodford Shale Formation was chosen for the fractured interval. In the area of investigation, it is buried at about 12,000 ft and varies in thickness between 100 and 400 ft. In addition, a flat horizon was introduced below the Woodford. The Woodford unit is a gently dipping event, and as such, this flat horizon introduced a wedge with varying thickness below the Woodford. We assigned three different anisotropy parameters to the wedge for simplification. The wedge was used to perform a sensitivity test to determine at which depth interval, level of anisotropy, and layer thickness of the fractured rock unit the velocity variation with azimuth

[1]Devon Energy Corp., Oklahoma City, Oklahoma, USA. E-mail: marianne.rauch-davies@dvn.com; david.langton@dvn.com.
[2]SeismicCity Inc., Houston, Texas, USA. E-mail: mbradshaw@seismiccity.com; abartana@seismiccity.com; dkosloff@seismiccity.com; jcodd@seismiccity.com; dkessler@seismiccity.com.
[3]Cimarex Energy Co., Tulsa, Oklahoma, USA. E-mail: jamier@cimarex.com.
[4]University of Calgary, Department of Geoscience, Calgary, Alberta, Canada. E-mail: margrave@ucalgary.ca.

effect becomes detectable. The model was simulated using anisotropic elastic 3D seismic forward modeling.

Orthorhombic medium

Azimuthal variations in velocity occur in the presence of an ordered heterogeneity on a scale much smaller than the wavelength of the propagating waves. Due to the layered nature of sedimentary basins, most show at least VTI, with faster velocities when particle motion is in the plane of the layering. Orthorhombic (ORT) symmetry induced by vertical fractures is the simplest expected cause of azimuthal anisotropy in sedimentary basins and would occur with a vertical plane of symmetry in the otherwise layered media.

In an ORT medium, symmetry is characterized by two sets of vertical planes, one parallel to the planes of the cracks and one perpendicular to the cracks. The direction of the planes can vary spatially. We use an X_1, X_2, X_3 coordinate system in which X_3 points in the vertical direction, and X_1 denotes the direction perpendicular to the crack planes. Azimuthal variations in V_{NMO} are expected to occur if an ORT symmetry exists within a layer. Thomsen's parameters for VTI material were extended to ORT symmetry by Tsvankin (1997). In terms of the elastic constants they are given as:

$$V_{P0} = \frac{\sqrt{C_{33}}}{\rho}; \qquad V_{S0} = \frac{\sqrt{C_{55}}}{\rho}$$

$$\varepsilon_1 = \frac{C_{22} - C_{33}}{2C_{33}}; \qquad \varepsilon_2 = \frac{C_{11} - C_{33}}{2C_{33}}$$

$$\gamma_1 = \frac{C_{66} - C_{55}}{2C_{55}}; \qquad \gamma_2 = \frac{C_{66} - C_{44}}{2C_{44}}$$

$$\delta_1 = \frac{(c_{23} + c_{44})^2 - (c_{33} - c_{44})^2}{2c_{33}(c_{33} - c_{44})}$$

$$\delta_2 = \frac{(c_{13} + c_{55})^2 - (c_{33} - c_{55})^2}{2c_{33}(c_{33} - c_{55})}$$

$$\delta_3 = \frac{(c_{12} + c_{66})^2 - (c_{11} - c_{66})^2}{2c_{11}(c_{11} - c_{66})}$$

The ϵ^2 and ϵ^1 parameters are related to the ratio of vertical P-wave velocity to the horizontal P-wave velocity on the vertical symmetry planes X_1–X_3 and X_2–X_3, respectively. Similarly, γ_2 and γ_1 relate SH velocity ratios on these planes. δ_2 and δ_1 influence moveout velocity at small reflection angles. δ_3 is related to the anisotropy on the horizontal X_1–X_2 plane. The elastic ORT model used in the study described here was constructed using this formulation.

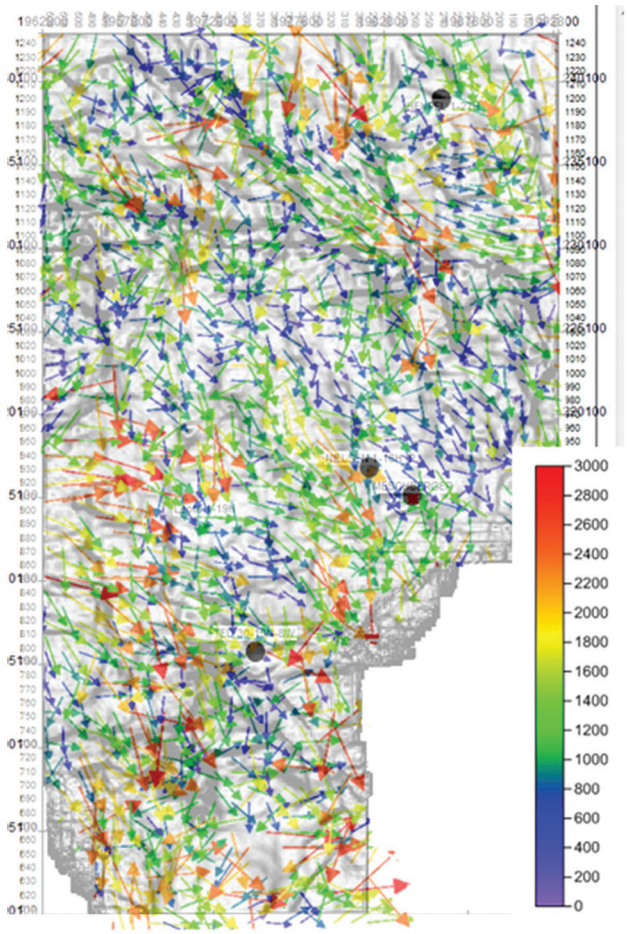

Figure 1. Arrow plots showing V_{fast}–V_{slow} generated by one of the participating vendors (Rauch-Davies and Sutherland, 2016) for the Woodford Formation. The arrows represent the orientation of the fast velocity. The magnitude of velocity difference V_{fast}–V_{slow} is represented in colors. The gray background shows the curvature attribute, which is an excellent geometric property for fault interpretation.

Model

Following an active development drilling program in the Woodford Shale Formation, we designed a model to test whether ORT anisotropy is measurable in ideal noise-free data and, if the answer is affirmative, to determine the limits on burial depth, interval thickness, and degree of anisotropy for which the fracture density and orientation is detectible. The model was constructed based on six horizons interpreted from a prestack depth-migrated (PSDM) 3D seismic survey in the Anadarko Basin, Oklahoma, USA (Figure 2). The layer of interest for the azimuthal characterization is the Woodford Shale. It has an average thickness of 250 ft

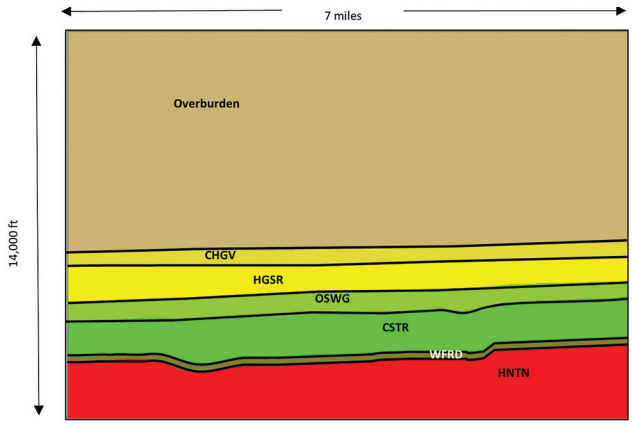

Figure 2. Geologic model constructed from a 3D PSDM data set in the Anadarko Basin, Oklahoma.

and varies in depth from 11,800 to 12,200 ft. The layers above the Woodford are assigned VTI parameters derived from log data, which are constant within each layer. The structural dips are small. Thus, any measurable azimuthal variation in residual moveout in this model can only be attributed to the anisotropy in the target layer and not to velocity heterogeneity or structure in the layers above the Woodford Formation.

As a control, we constructed a base model with all layers, including the Woodford, having only VTI anisotropy. The target layer was then modified to have ORT anisotropy. A flat layer that produced a wedge of progressively increasing thickness and constant ORT anisotropy was also placed in the deepest layer to provide control on the minimum necessary thickness for identification of azimuthal variations in V_{NMO} in our modeled scenario.

For the VTI model, a δ_1 value of 12% was chosen for the Woodford Formation. For the shale layer in the ORT model, the slow axis δ_1 was set at 6% and the fast axis δ_2 was variable to give a desired azimuthal variation in V_{NMO}. Table 1 provides the properties of each layer of the model. The other VTI parameters were kept constant, and the other ORT parameters (i.e., δ_3) were calculated to ensure physical consistency of the model. To design a variable model that can be used for data analysis, we constructed a series of anisotropic tiles in the target layer. Figure 3 shows a map view of the effective V_{NMO} anisotropy and represents the difference between δ_1 and δ_2. Table 2 provides the anisotropy and azimuth values. Azimuth is the direction of the X_2 axis relative to north. To test the extremes of azimuthal sensitivity, a flat reflector below the Hunton was added to the ORT model. With the dip of the Woodford to Hunton interval

Table 1. Model parameterization: velocity, density, and anisotropy properties.

Unit	P vel ft/s	S vel ft/s	Density gr/m³	δ_1 %	ϵ_1 %	γ_1 %
OVBN	10,500 to 13,000	7000 to 8450	2.3	2	7	7
CHGV	13,400	8710	2.5	5	15	15
HGSR	13,500	8775	2.6	8	19	19
OSWG	13,700	8905	2.7	9	17	17
CSTR	14,000	9100	2.6	4	9	9
WFRD	11,500	7475	2.35	12	17	17
HNTN	14,000	9100	2.7	2	5	5

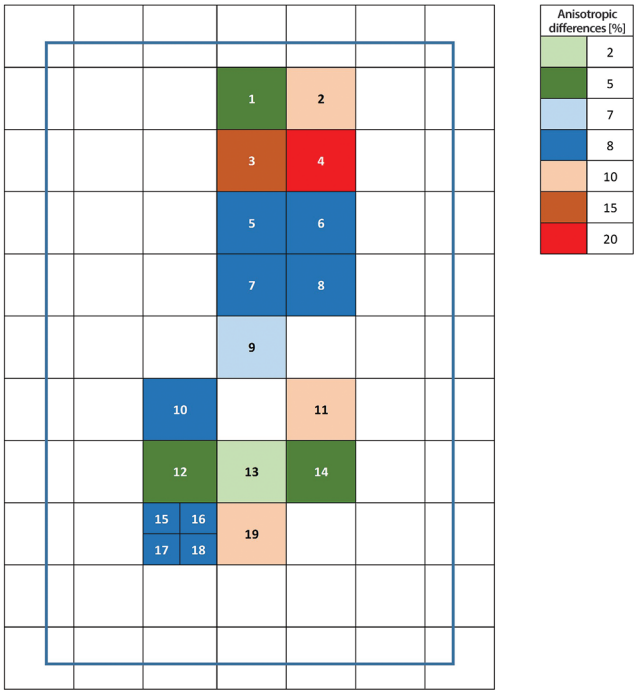

Figure 3. Map view of the effective V_{NMO} anisotropy embedded in the Woodford Shale layer.

Table 2. ORT model parameterization: anisotropic values and azimuthal orientation within each individual tile as shown in Figure 3. Orientation is clockwise from north.

Tile no.	Fracture orientation in degrees	Anisotropic differences in %
1	40	5
2	40	10
3	40	15
4	40	20
5	20	8
6	150	8
7	90	8
8	40	8
9	0	7
10	90	8
11	40	10
12	100	5
13	30	2
14	40	5
15	20	8
16	150	8
17	90	8
18	40	8
19	40	10

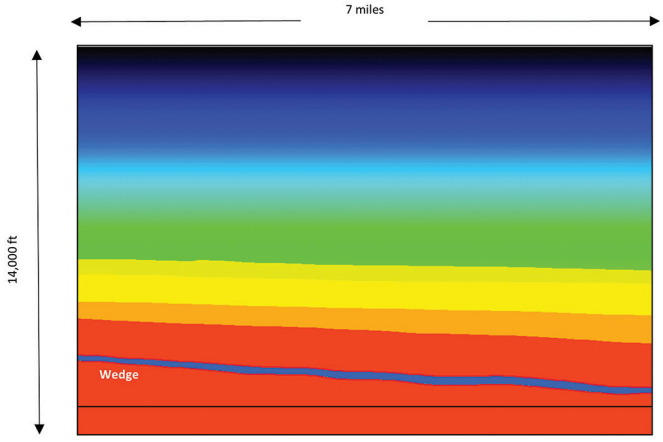

Figure 4. Deep wedge was added to the model to create an additional layer with variable thickness.

above, this formed a naturally thickening wedge from about 200 to 2000 ft thickness. The wedge was divided into three sections of low anisotropy (2%), medium anisotropy (5%), and high anisotropy (8%). The geologic model including the deep wedge is shown in Figure 4.

Method

Generation of the synthetic seismic data was accomplished with an elastic anisotropic simulator (Carcione, 2001). Acquisition parameters were chosen to represent what is typical of a modern wide-azimuth land survey. The source function was designed using a broadband Butterworth filter over a frequency band typical for this area — i.e., 0–60 Hz. Figure 5 shows an example simulated shot gather generated in the elastic anisotropic simulation. The survey size was 11 × 9 miles. Shot locations were optimized to produce uniform fold with shot inline distance of about 660 ft and shot line spacing of about 770 ft. The acquisition patch size was 24,970 × 23,430 ft. Receiver spacing was 110 ft, and receiver cable spacing was 330 ft. This resulted in 228 receivers per cable and 72 cables per recording patch with minimal offset of 78 ft and maximum offset of 17,196 ft. The shot and receiver acquisition design resulted in uniform fold distribution with up to a maximum of 98 fold as well as uniform distribution of offset and azimuth.

The simulated data set for both the VTI model and the ORT model were prestack time and depth migrated using VTI Kirchhoff summation algorithms. Figure 6 shows a section from the PSDM volume. The migration velocity was the VTI velocity model. Migrated data were output with 18 azimuth sectors of 10° each and with offsets ranging from 100 to 17,100 ft. This produced 20 offset classes per common-depth point with 850 ft distance between offset classes. The output common-offset variable-azimuth (COVA) gathers resulted in a nominal fold of 360. For analysis, the residual moveout on the migrated COVA gathers was measured and analyzed.

Results and analysis

To analyze the PSDM results, both data inspection and azimuthal velocity analysis were performed. Figure 7 shows a depth cross section of the model with an annotated inspection location. A COVA depth-migrated gather was extracted at the highlighted location and analyzed (Figures 8–10).

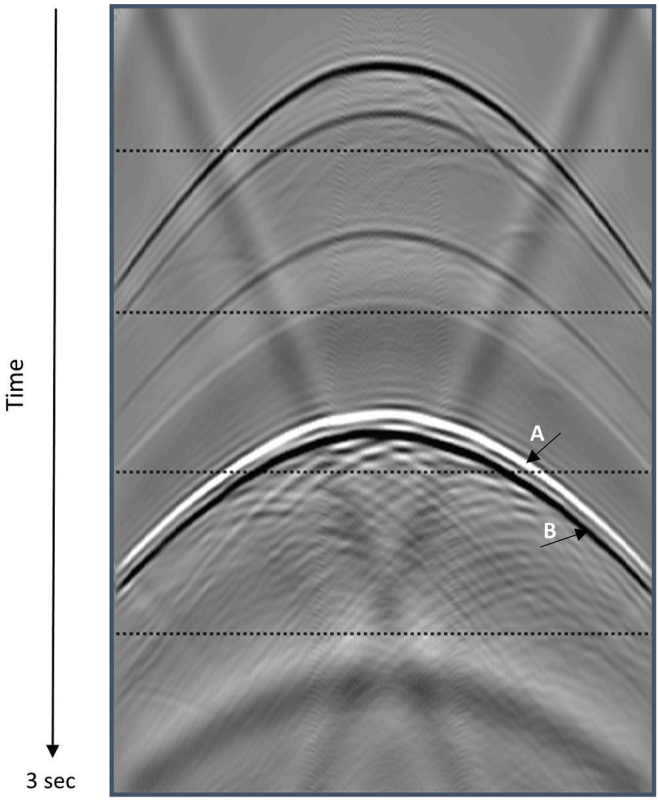

Figure 5. Simulated shot gather. Event A is the reflection from top of the Woodford Formation. Event B is the reflection from the top of the Hunton interval, which is the base of Woodford.

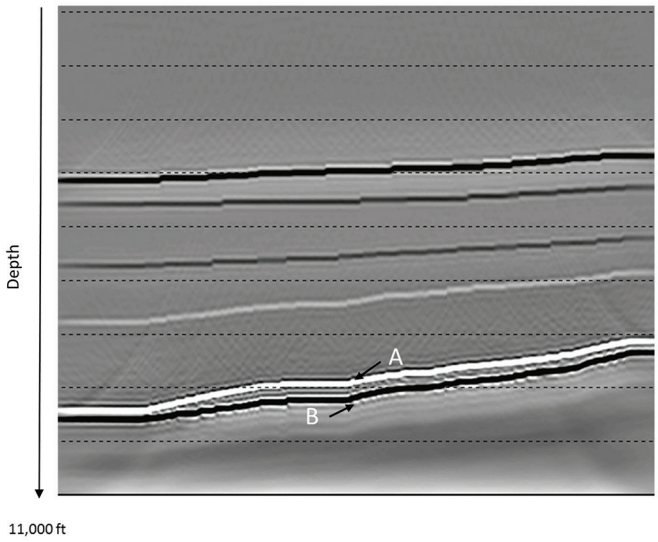

Figure 6. PSDM crossline of the elastic simulated data. Annotation A is the top of the Woodford layer, and B is the top of the Hunton.

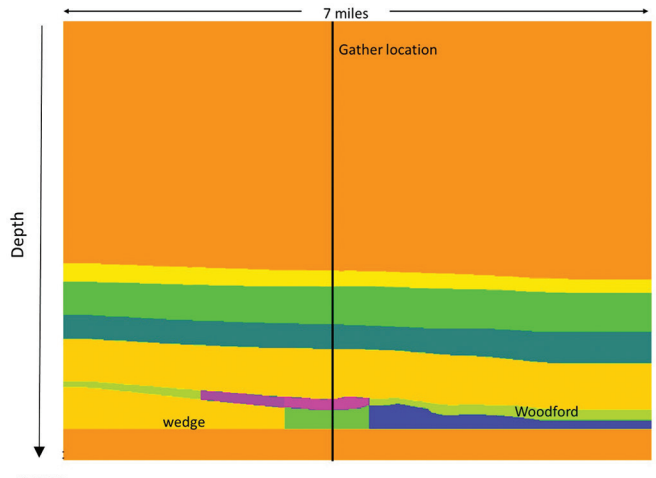

Figure 7. Cross section of the anisotropic model. Annotated (black line) is the location used for analysis of the COVA gather shown in Figures 8–10. The top of the shale layer is the Woodford marker and the base of the shale layer is the Hunton marker. Colors within the Woodford represent various degrees of anisotropy. At this location, the anisotropy is 5%, the Woodford thickness is 345 ft, and the thickness of the wedge layer is 600 ft.

Figure 8 illustrates the VTI COVA PSDM gather migrated using the VTI simulated data set at the annotated location and the amplitude picked within the yellow rectangle. The Woodford and Hunton horizons are shown in blue and green, respectively.

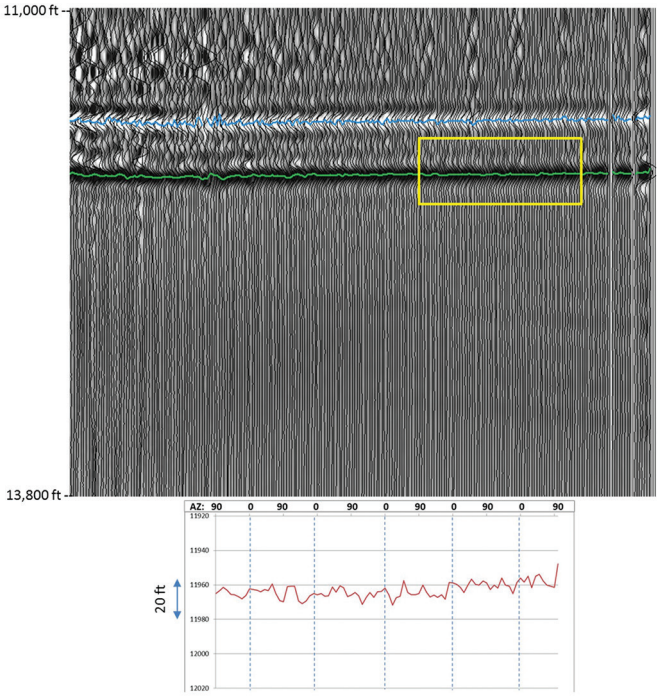

Figure 8. PSDM COVA gather generated using VTI model. Blue horizon is Woodford, green horizon is Hunton (i.e., base Woodford), yellow rectangle is analysis window for lower display that shows the depth anomalies of the Hunton reflector over this interval.

Since the input model for the simulation was VTI, as expected, no sinusoidal moveout behavior is present, and the small variations along the Hunton interface are attributed to noise.

Figures 9 and 10 display the VTI PSDM COVA gather migrated using the ORT simulated data set. Figure 9 examines the gather at the base of shale layer (i.e., Hunton). At the analysis location, the Woodford is 345 ft thick and has a modeled anisotropy of 5%. This is below resolution, and negligible sinusoidal behavior is evident. Figure 10 examines the gather at the base of the wedge. An examination of the COVA gather at the analysis location shows that detectable sinusoidal amplitude variation can be observed at the wedge interface where the anisotropic layer is 600 ft thick and the anisotropy value is 5%. The displacement, however, is about plus/minus 20 ft, which in real data is most likely too small to be measurable.

Figures 11 and 12 show the Woodford and wedge thickness with the anisotropy model geometry as overlays. The Woodford slopes upward toward the northeast and thins at the same time. The wedge is a straight line below the Woodford interface and as such is thicker toward the northeast.

To compare to the real data V_{fast}–V_{slow} map shown in Figure 1, we calculated V_{fast}–V_{slow} maps using the simulated PSDM COVA gathers (Grechka and Tsvankin, 1999). This was done for the base of the Woodford (i.e., top Hunton) layer and for the wedge layer. Figure 13 displays the V_{fast}–V_{slow} vector map (i.e., arrow plots) for the shale (i.e., Woodford) interval after PSDM. Figure 14 displays the V_{fast}–V_{slow} vector map (i.e., arrow plots) for the wedge interval after PSDM. The color and length of the arrows are linked to the strength of the anisotropic behavior, while the arrow itself indicates the fast direction — i.e., direction

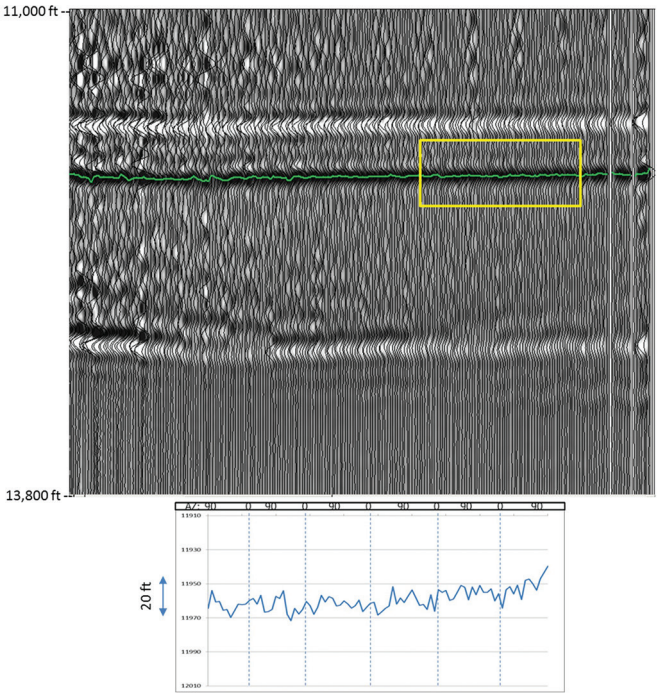

Figure 9. PSDM COVA gather generated using the ORT model. The green horizon represents the base of the Woodford, top of Hunton reflector. The yellow rectangle shows the analysis window for the lower graph. This graph displays the event depth variation along the chosen window. No sinusoidal behavior can be detected.

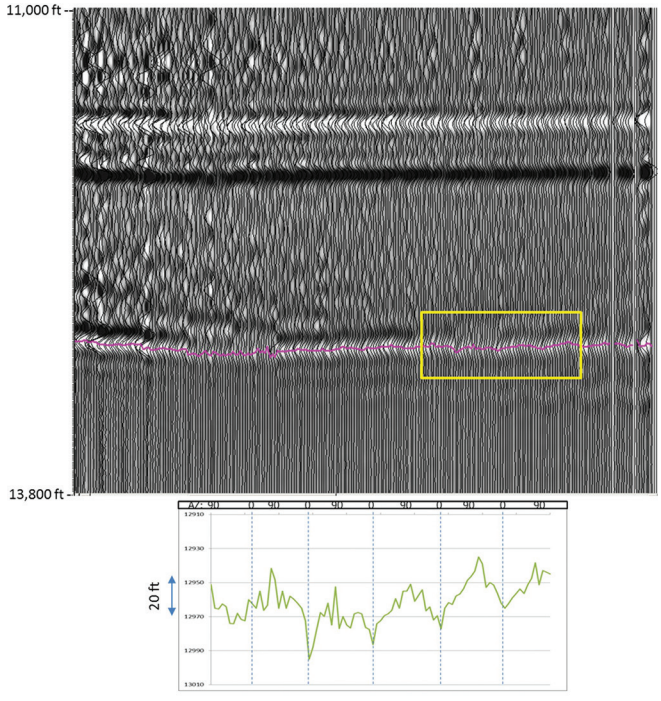

Figure 10. PSDM COVA gather generated using the ORT model. The pink horizon represents the wedge and the yellow rectangle the area over which the lower graph was calculated. Sinusoidal behavior can be detected. The displacement is in the order of plus/minus 20 ft.

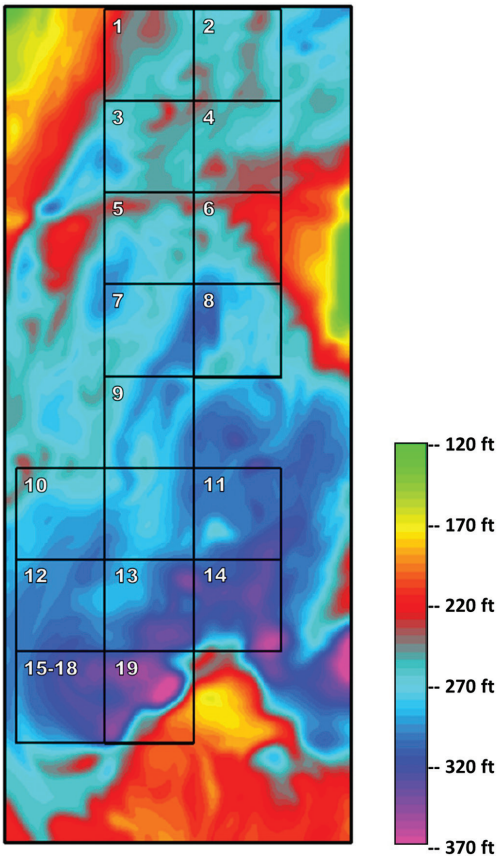

Figure 11. Woodford layer thickness with ORT anisotropy model geometry as overlay.

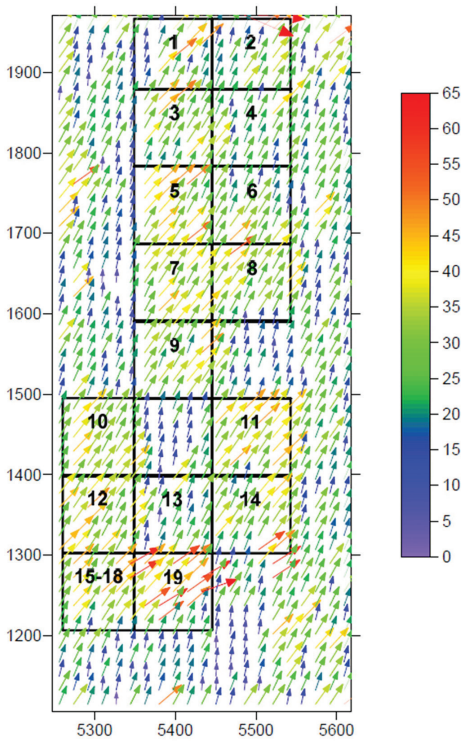

Figure 13. V_{fast}–V_{slow} arrow map generated from the PSDM of the ORT data set for the Woodford Shale. The direction of the arrow indicates the direction of anisotropy and the color represents the velocity difference in ft/s. The black outlines refer to the areas denoted on Figure 3, which represents the ORT anisotropic model geometry.

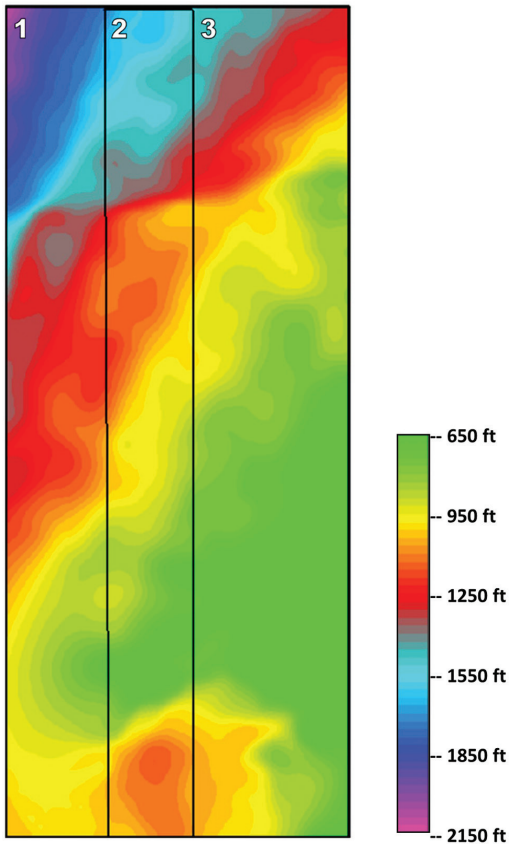

Figure 12. Wedge layer thickness with model ORT anisotropy geometry as overlay.

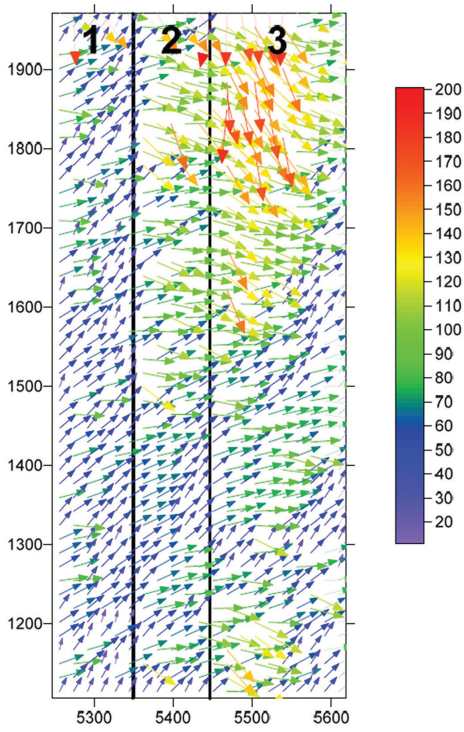

Figure 14. V_{fast}–V_{slow} arrow map generated from the PSDM of the ORT data set for the wedge layer. The direction of the arrow indicates the direction of anisotropy and the color represents the velocity difference in ft/s. The black outlines refer to the areas denoted on Figure 3, which represents the ORT anisotropic model geometry.

of fracturing, dominant direction of anisotropy. The overlaying grid exhibits the modeled anisotropic geometry.

At the Woodford interval, the $V_{fast}-V_{slow}$ measured in feet per second is at its maximum 65 ft/s. A correlation is present between the ORT model (shown in Figure 3) and the calculated results after PSDM, but these variations are insignificant. The $V_{fast}-V_{slow}$ at the wedge interval is larger but still small when compared to the interval velocities (on the order of 14,000 ft/s).

Conclusions

Azimuthal variations in V_{NMO} or migration velocity are routinely observed from processed seismic data. Correcting for this effect often shows substantial uplift in the stacked image. The interpretation of this variation as due to intrinsic anisotropy in the form of vertical fractures or stress-induced heterogeneity is common in the industry. Significant evidence suggests that these azimuthal variations are not always due to intrinsic anisotropy and are highly dependent on reservoir layer thickness, burial depth, and strength of anisotropy. Yet there is a strong persistence of this interpretation. To address this issue, we built a model with varying levels of intrinsic VTI and ORT anisotropy, following the Woodford Formation in the Anadarko Basin in Oklahoma. This shale interval is at a depth of approximately 12,000 ft and varies in thickness between 150 and 450 ft in our area of interest. To investigate the link between layer thickness and the sinusoidal behavior, we added a flat horizon below the Woodford. As the Woodford gently dips to the south, this layer generates a wedge with thickness variations from about 250 to 2000 ft. This enabled testing the ability to detect azimuthal anisotropy over a layer of variable thickness. We modeled three different percentages of anisotropy within this artificial layer, varying from 2% to 8%.

For the relatively thin Woodford Formation in the study area, results at the Hunton (i.e., base Woodford) interval show a very small moveout variation even over areas with higher modeled anisotropy and larger layer thickness. The values are between 5 and 65 ft/s (equivalent to 0.5% maximum velocity variation), which at this depth is not detectable from seismic data. Analysis of the seismic data for the thicker modeled wedge layer shows velocity variation from about 20 to 200 ft/s (equivalent to 1.5% maximum velocity variation) in areas with larger layer thickness and higher anisotropy. This indicates that even with relatively high levels of azimuthal anisotropy in a thin layer as the Woodford Shale in the Anadarko Basin (several hundred feet thick at a typical reservoir depth), azimuthal variations in depth-migration velocity are undetectable.

The conclusions of the study on the inability to resolve fracture orientation and density for the relatively thin Woodford Shale Formation are in agreement with observations made using real data in the Anadarko Basin. The current test model does not include lateral velocity variations in the layers, has very small dips, and the elastic simulation did not include attenuation and dispersion. Furthermore, the PSDM applied in this study was conducted using a known model. With real data, these factors will further obscure the fracture signature, especially in thin, deep target layers. It is possible that much of the azimuthal variation in velocities that we observe in real data sets is due to lateral velocity heterogeneity not properly accounted for in time and even depth migration. TLE

Acknowledgments

We thank Devon Energy for the opportunity to pursue this work and approval to bring it to publication.

Data and materials availability

Data associated with this research are confidential and cannot be released.

Corresponding author: dkessler@seismiccity.com

References

Carcione, J. M., 2001, Wave fields in real media: Wave propagation in anisotropic, anelastic and porous media: Pergamon.

Cherif, B., A. Zarkhidze, N. Meddour, H. F. Zeidan, C. Chironi, H. Harkas, and A. Widjiastono, 2016, Apparent azimuthal anisotropy resolved by depth imaging: 86th Annual International Meeting, SEG, Expanded Abstracts, 328–331, https://doi.org/10.1190/segam2016-13948733.1.

Grechka, V., and I. Tsvankin, 1999, 3-D moveout velocity analysis and parameter estimation for orthorhombic media: Geophysics, **64**, no. 3, 820–837, https://doi.org/10.1190/1.1444593.

Lynn, W., 2007, Uncertainty implications in azimuthal velocity analysis: 77th Annual International Meeting, SEG, Expanded Abstracts, 84–88, https://doi.org/10.1190/1.2792387.

Lynn, W., 2011, Azimuthal interval velocity uncertainty: 81st Annual International Meeting, SEG, Expanded Abstracts, 279–283, https://doi.org/10.1190/1.3627776.

Rauch-Davies, M., and S. Sutherland, 2016, Azimuthal full anisotropic PSTM for image improvement and mapping of small scale discontinuities using anisotropic velocity attributes: 86th Annual International Meeting, SEG, Expanded Abstracts, 5264–5268, https://doi.org/10.1190/segam2016-13861751.1.

Rich, J., B. Kennedy, and M. Rauch-Davies, 2016, Understanding azimuthal P-wave anisotropy through multiple vendor and attribute comparisons: Unconventional Resources Technology Conference, https://doi.org/10.15530/URTEC-2016-2423045.

Tsvankin, I., 1997, Anisotropic parameters and P-wave velocity for orthorhombic media: Geophysics, **62**, no. 4, 1292–1309, https://doi.org/10.1190/1.1444231.